J Nanopart Res (2021) 23: 117
https://doi.org/10.1007/s11051-021-05203-7

RESEARCH PAPER

Magnetic moment and volume fraction controlling chain-like structures of magnetic nanoparticles in uniform magnetic fields

Yongpeng Chen · Jianguo Zhang · Huichao Zhang · Zunning Zhou

Received: 29 September 2020 / Accepted: 3 April 2021 / Published online: 17 May 2021

Abstract The magnetically assembled chain-like structures of magnetic nanoparticles attract great attention due to their unique properties. In this paper, we studied the influences of essential magnetic controlling parameters on the chain-like structures of magnetic nanoparticles with diameter $d = 360$ nm using a 3D Monte Carlo simulation. The magnetic moment and volume fraction of magnetic nanoparticles were found to play crucial roles in the arrangement of the nanoparticles. The simulation results were in agreement with experimental evidence, summarized as follows: In the limit of low magnetic moment $m < 3.7\times10^{-16}$ A·m^2, magnetic nanoparticles did not linearly arrange along the direction of the magnetic field but formed aggregates. At magnetic moment $m > 1.5\times10^{-15}$ A·m^2 and volume fraction $\varphi<0.02\%$, the formation effect of nanochains consisting of individual particles was first enhanced and then remained almost unchanged with increasing magnetic moment. For magnetic moment $m>7.3\times10^{-15}$ A·m^2 and volume fraction $\varphi>1\%$, nanochains gradually coarsened into the nanobundles with increasing volume fraction. The results can provide a theoretical basis to construct and regulate other assembled structures consisting of building blocks.

Keywords Magnetic nanoparticles · Monte Carlo simulation · Chain-like nanoparticle structures · Magnetic moment · Volume fraction

Y. Chen · J. Zhang · H. Zhang · Z. Zhou (✉)
State Key Laboratory of Explosion Science and Technology, Beijing Institute of Technology, Beijing 100081, China
e-mail: zzn@bit.edu.cn

Introduction

Magnetic nanoparticles exposed to external magnetic fields can assemble into ordered structures including one-dimensional (1D) nanochains, 2D sheets, and 3D photonic crystals (He et al. 2012; Wang et al. 2013a, b; Ohno et al. 2018; He et al. 2011; Zhang et al. 2010; Helseth 2005). 1D chain-like structures represent the simplest ordered distribution when magnetic nanoparticles transform from a random state. The shape anisotropy and periodic structures give 1D nanostructures obvious advantages in potential applications such as microelectronics, magnetic recording, drug delivery, sensing, interference, photovoltaic, spintronics, etc. (Helseth 2005; Yuan et al. 2011; Laughlin et al. 2000; Kamble and Mathe 2008; Richardson and Jones 2009; Chen et al. 2018; Ravi and Prabvin 2013; Ravi and Shashikanth 2017).

Driven by the excellent performance and broad application prospects, considerable efforts have been devoted to magnetic assembly of chain-like structures, including experimental observations and numerical simulations (Kralj and Makovec 2015; Wang et al. 2010; Ye et al. 2010; Hu et al. 2011; Wang et al. 2013a, b; Satoh et al. 1996, 2000; Enomoto et al. 2003; Peng et al. 2009; Xue et al. 2017). Prior work has been carried out to reveal the assembly mechanism in colloidal suspensions (Tran et al. 2015; Furst and Gast 2000; Bertoni et al. 2011; Lalatonne et al. 2004). The key factors that determine the chain-like structures of magnetic nanoparticles are two major types of interactions: van der Waals and magnetic dipolar interactions. Under weak

dipolar interactions, such as magnetic nanocrystals, van der Waals interactions are expected to be the dominant contribution to the total interparticle potential, so isotropic van der Waals interactions induce the formation of disordered aggregates. Under weak van der Waals interactions, dominant dipolar interactions can control the formation of chain-like structures of individual nanoparticles. Furthermore, the interparticle interactions depend on magnetic controlling parameters, such as the magnetic field intensity, magnetization, particle radius and concentration (Xue and Furlani 2014, 2015). However, research on the magnetic assembly mechanism is mainly from the perspective of interparticle interactions, and the quantitative relationship between essential magnetic controlling parameters and assembled chain-like structures still needs to be further studied.

In this work, we use a Monte Carlo method to simulate the chain-like structure formation of magnetic nanoparticles. The aim is to investigate the influences of essential magnetic controlling parameters on chain-like structures in theory. The results presented here are in agreement with the experimental observations of assembled chain-like structures, suggesting the possibility of guiding the construction of other assembled structures consisting of building blocks.

Methods

Experiment

$MnFe_2O_4$ nanospheres were obtained by the solvothermal method. The preparation procedure and characterization results are described in detail in the Supplementary Material. In addition, the synthesis process of the chain-like structures was presented as follows. A total of 1.5 mL of $MnFe_2O_4$ aqueous solution was dispersed in ethanol (10 mL) and tetraethoxysilane (TEOS, 50 μL) under sonication. After that, the mixture was transferred into a flask under mechanical stirring. After 12 min, aqueous ammonia (0.5 mL) was quickly injected, and then the mixture was transferred to a beaker (25 mL) and placed inside a Helmholtz coil creating a uniform magnetic field for 1 h. The magnetically assembled structure was stabilized and fixated by the deposition of an additional layer of silica using the hydrolyzation and condensation of TEOS. After being removed from the magnetic field, the sample was allowed to sit undisturbed for another 30 min, after which it was washed with ethanol three times and redispersed in ethanol.

Calculation

Simulations were carried out using a three-dimensional Monte Carlo method based on the Metropolis algorithm (Peng et al. 2009). The Monte-Carlo method is a statistical tool that models the probability of different outcomes and has been used to analyze magnetic properties and the Curie temperature (Miller and Drillon 2005; Ravi 2020). The simulation system consisted of N = 200 particles with diameter d dispersed in a 3D cube. The particles were covered by a steric layer of thickness $\delta = 0.01d$. The initial configuration of particles was taken as random. The maximum displacement of a particle in one trial move was $0.025d$, and a cluster was defined as a group of particles in which adjacent particles existed within $1.025d$. The moments of magnetic particles were fixed along the field direction. Periodic boundary conditions were applied in the X, Y and Z directions. Each simulation was carried out up to 20,000 steps to obtain a stable assembled structure.

Our computational model took into account several dominant assembly mechanisms, including the induced magnetostatic energy $u_i^{(H)}$, magnetic dipole-dipole interactions $u_{ij}^{(m)}$, van der Waals potential energy $u_{ij}^{(v)}$ and surfactant interaction $u_{ij}^{(r)}$ caused by surfactant-surfactant contact. The details of the model are briefly summarized as follows (Xue et al. 2017):

$$u_i^{(H)} = -\mu_o \mathbf{m_i} \cdot \mathbf{H} \tag{1}$$

$$u_{ij}^{(m)} = \frac{\mu_o}{4\pi r_{ij}^3} \cdot \left[\mathbf{m_i} \cdot \mathbf{m_j} - \frac{3}{r_{ij}^2} \left(\mathbf{m_i} \cdot \mathbf{r_{ij}} \right) \left(\mathbf{m_j} \cdot \mathbf{r_{ij}} \right) \right] \tag{2}$$

$$u_{ij}^{(v)} = -\frac{A}{6} \left[\frac{2R_{p,i} \cdot R_{p,j}}{r_{ij}^2 - \left(R_{p,i} + R_{p,j}\right)^2} + \frac{2R_{p,i} \cdot R_{p,j}}{r_{ij}^2 - \left(R_{p,i} - R_{p,j}\right)^2} + \ln \frac{r_{ij}^2 - \left(R_{p,i} + R_{p,j}\right)^2}{r_{ij}^2 - \left(R_{p,i} - R_{p,j}\right)^2} \right] \tag{3}$$

$$u_{ij}^{(r)} = 2\pi \frac{R_{p,i}^2 \cdot R_{p,j}^2}{\left(R_{p,i} + R_{p,j}\right)^2} N_s k_B T \left[2 - \frac{r_{ij} - \left(R_{p,i} + R_{p,j}\right)}{\delta} - \frac{r_{ij}}{\delta} \ln\left(\frac{\left(R_{p,i} + R_{p,j}\right) + 2\delta}{r_{ij}}\right)\right] \quad (4)$$

where μ_o is the magnetic permeability of free space, **H** is the applied magnetic field, $\mathbf{m_i}$ and $\mathbf{m_j}$ are the magnetic moments of the *i*'th and *j*'th particles, $R_{p,\,i}$ and $R_{p,\,j}$ are the radii of the *i*'th and *j*'th particles, respectively (in our study, $R_{p,\,i}$=$R_{p,\,j}$), r_{ij} is the magnitude of the vector $\mathbf{r_{ij}}$ drawn from particle *i* to *j*, *A* is the Hamaker constant, k_B is Boltzmann's constant, *T* is the absolute temperature of the suspension, δ is the thickness of the surfactant layer and N_s is the surface density of surfactant molecules.

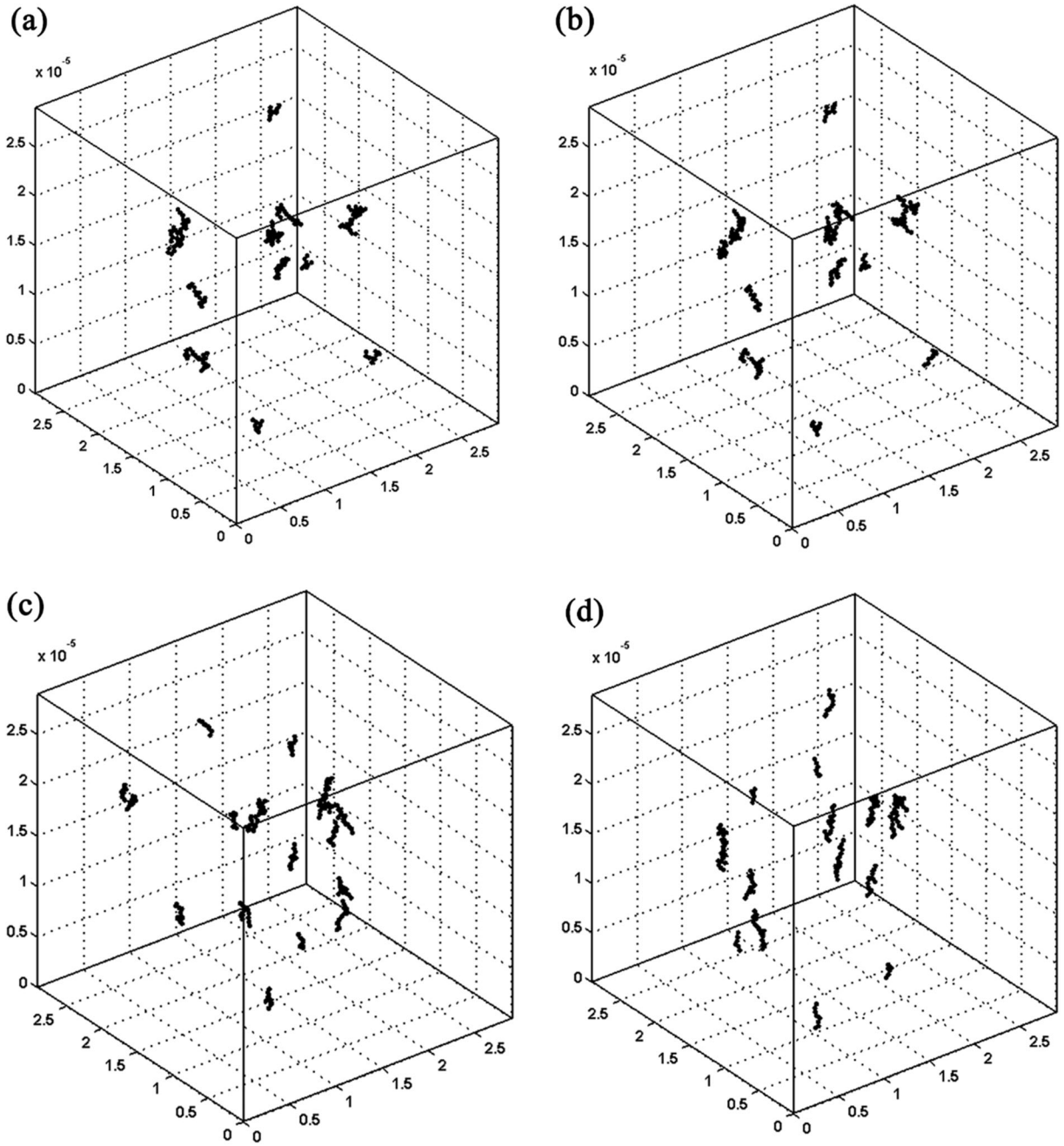

Fig. 1 Assembled structure of magnetic nanoparticles for φ= 0.02% and d = 360 nm: (a) $m = 2.2\times10^{-16}$ A·m^2; (b) $m = 2.4\times10^{-16}$ A·m^2; (c) $m = 2.9\times10^{-16}$ A·m^2; (d) $m = 3.7\times10^{-16}$ A·m^2

Results and discussion

From the mathematical expression of the interaction model, the factors that influence the interactions determining the assembled structures are the radius of particles R, magnetic moment of particles m, center-center distance between particles r determined by the volume fraction of particles φ, and magnetic field intensity H.

An applied magnetic field induces a magnetic moment in a magnetic particle $m=\chi HV=MV$ (Wang et al. 2013a, b), where χ is the volume susceptibility of the particle, H is the local magnetic field intensity, M is the magnetization intensity of the particle, and V is the volume of the particle. For magnetically assembled systems, the radius of particles R and magnetic field intensity H control assembled structures mainly by influencing the magnetic moment m. Hence, the major magnetic controlling parameters are the magnetic moment m and volume fraction φ of particles. The effects of the magnetic moment and volume fraction on the assembled chain-like structures are discussed in the following section.

Aggregates of magnetic nanoparticles

According to the magnetic moment $m = MV$, we can adjust the magnetic moment by changing the magnetization intensity. The assembled distributions of magnetic nanoparticles at low magnetic moments were studied, using snapshots of the assembled structures in equilibrium for $\varphi = 0.02\%$, $d = 360$ nm, and $M = 9$ kA/m, 10 kA/m, 12 kA/m, and 15 kA/m, namely the magnetic moment was $m=\frac{1}{6}\pi M d^3=2.2\times10^{-16}$ A·m^2, 2.4×10^{-16} A·m^2, 2.9×10^{-16} A·m^2, and 3.7×10^{-16} A·m^2, as shown in Fig. 1. At m = 2.2×10^{-16} A·m^2 and 2.4×10^{-16} A·m^2, which are low magnetic moments, magnetic nanoparticles did not arrange along the direction of the magnetic field but formed disordered aggregates as shown in the illustration of Fig. 1a and 1b. Figure 2 shows the TEM image of assembled disordered aggregates of magnetic nanoparticles for the stirring speed ω= 280 r/min, the volume fraction φ= 0.02%, the magnetic field intensity H = 3978.9 A/m, and the TEM image qualitatively supports the simulation results in Fig. 1a and 1b.

Upon further increasing the magnetic moment, magnetic nanoparticles gradually assembled into chain-like aggregates rather than nanochains of individual particles, as shown in Fig. 1c–1d. For a low magnetic moment, the value of the magnetic moment was too small to produce significant magnetic dipolar interactions. Therefore, van der Waals interactions were expected to be the dominant contribution to the total interparticle potential. Consequently, the individual magnetic nanoparticles formed aggregates due to the van der Waals interactions, and the strength of the dipole moment of aggregates can facilitate the formation of chain-like clusters.

Nanochain formation of individual magnetic nanoparticles

As the magnetic moment of the magnetic nanoparticles further increased, sufficient magnetic dipolar interactions versus van der Waals interactions were produced. As shown in Fig. 3a, the aggregates in the nanochains disappeared, and the clusters displayed the formation of nanochains of individual particles for $m = 1.5\times10^{-15}$ A·m^2, indicating that dipolar interactions overwhelmed

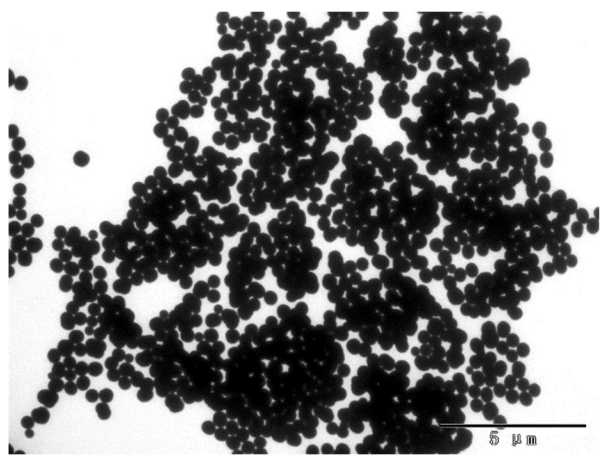

Fig. 2 TEM image of assembled disordered aggregates of magnetic nanoparticles for ω = 280 r/min, φ= 0.02%, H = 3978.9 A/m

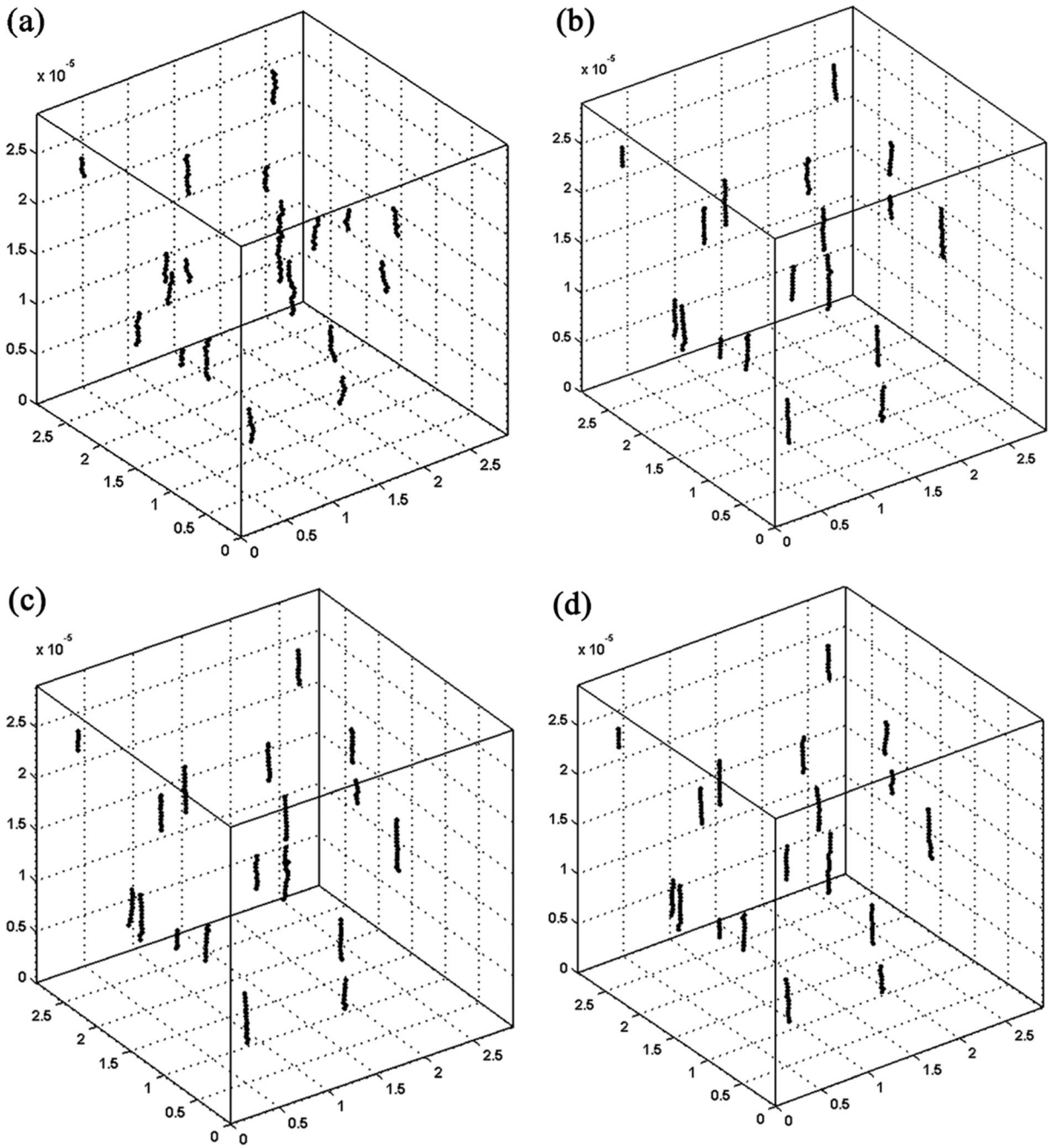

Fig. 3 Assembled structure of magnetic nanoparticles for φ= 0.02% and d = 360 nm: (a) $m = 1.5\times10^{-15}$ A·m^2; (b) $m = 7.3\times10^{-15}$ A·m^2; (c) $m = 9.8\times10^{-15}$ A·m^2; (d) $m = 1.2\times10^{-14}$ A·m^2

van der Waals interactions to drive the assembly of nanochains.

For the case of $m = 7.3\times10^{-15}$ A·m^2, the short nanochains gradually merged into long nanochains, and the arrangement of the nanochains became straighter, in agreement with the TEM image (ω= 280 r/min, φ= 0.02%, H = 19098.6 A/m) in Fig. 4. When the magnetization intensity further increased to $m = 9.8\times10^{-15}$ A·m^2 and even $m = 1.2\times10^{-14}$ A·m^2, the distribution of nanochains was almost the same as that in the case of $m = 7.3\times10^{-15}$ A·m^2 based on observing Fig. 3b–3d and comparing the curves in Fig. 5. This

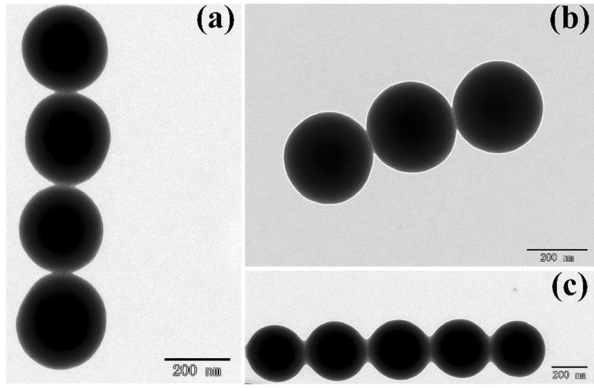

Fig. 4 TEM images of nanochains of individual magnetic nanoparticles for ω = 280 r/min, φ= 0.02%, H = 19098.6 A/m

occurred because at a high magnetic moment and a low volume fraction, the nanochains were too rigid and the dipolar interactions between nanochains were repulsive in the far field, making it difficult for these nanochains to interact to merge into longer nanochains (Furst and Gast 2000).

Transition from nanochains to nanobundles

At a high magnetic moment and a low volume fraction, the rigid nanochains with interchain repulsion interactions were dilute and well separated, and the distribution of chain-like assembled structures was mainly determined by the volume fraction. Hence, the assembly process of magnetic nanoparticles at high magnetic moment and volume fraction was investigated with m = 7.3×10^{-15} A·m^2, d = 360 nm, and φ= 1, 2, 6, and 8%. For reasons of computation time, the volume fraction of magnetic nanoparticles was adjusted by changing the side length of the computational domain.

Fig. 6 shows snapshots of the assembled structures in equilibrium. As the volume fraction of magnetic particles increased, the nanochains gradually attracted each other and coarsened into nanobundles, and these bundle-like structures were qualitatively in agreement with the experimental observation (ω= 280 r/min, φ= 8%, H = 19098.6 A/m) in Fig. 7. These results indicated that for dilute dipolar nanochains, the interchain interactions, mainly magnetic dipole-dipole repulsion interactions, kept the chains away from each other. However, at higher volume fractions, the separation between nanochains decreased, and the interchain repulsive interactions significantly increased. When the volume fraction of the nanochains, as well as the dipolar repulsive interactions increased to a certain extent, the interchain repulsive interactions were sufficiently strong such that the assembled system became thermodynamically unstable.

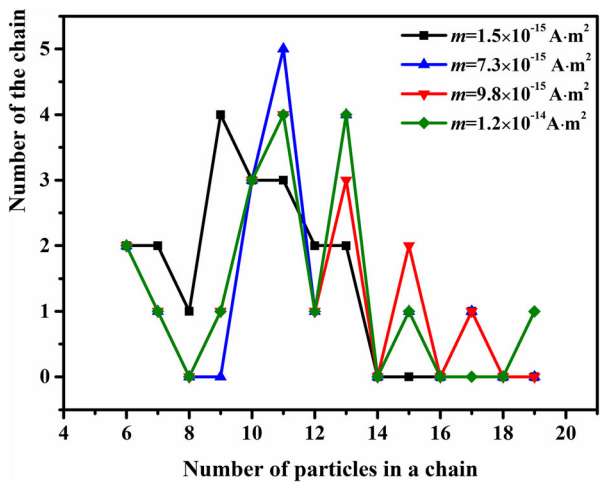

Fig. 5 Number distribution of particles in a chain

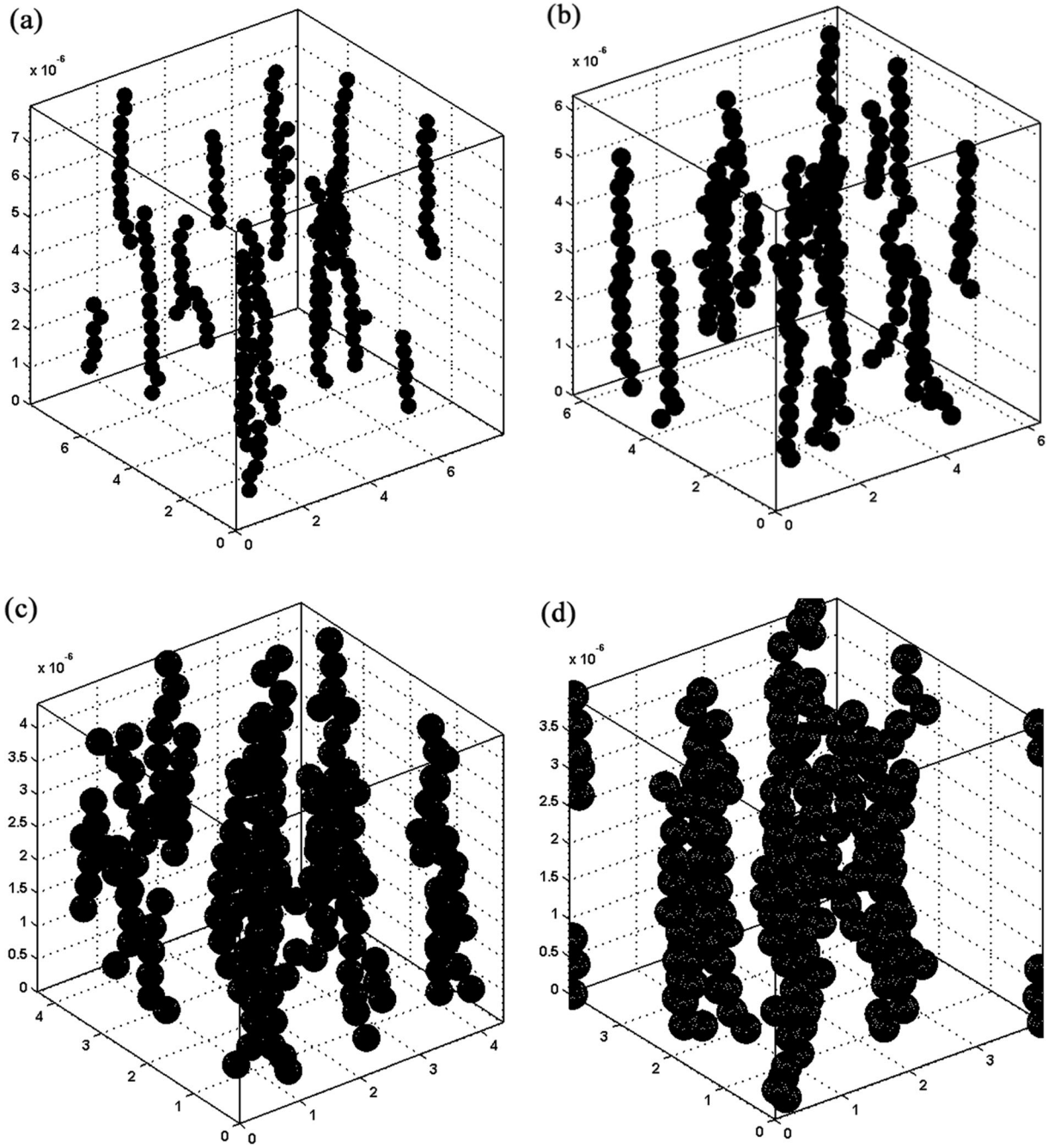

Fig. 6 Assembled structure of magnetic nanoparticles for $m = 7.3\times10^{-15}$ A·m^2 and $d = 360$ nm: (a) $\varphi = 1\%$; (b) $\varphi = 2\%$; (c) $\varphi = 6\%$; (d) $\varphi = 8\%$

Furthermore, the near-field behavior of fluctuating nanochains exhibited a strong and sudden change between attractive and repulsive interactions, resulting in a relative displacement between the nanochains, and the nanochains started to aggregate into nanobundles at this moment (Malik et al. 2012; Islam et al. 2003).

Conclusions

The influences of essential magnetic controlling parameters on the chain-like structures of magnetic nanoparticles were studied by making use of a Monte Carlo 3D algorithm. The magnetic moment and volume fraction

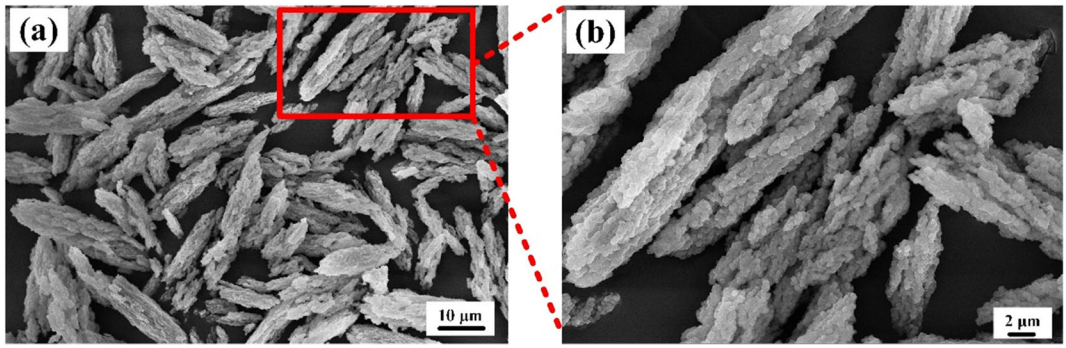

Fig. 7 SEM images of 3D nanobundles for ω = 280 r/min, φ= 8%, H = 19098.6 A/m

of magnetic nanoparticles were found to play crucial roles in the arrangement of the nanoparticles. The simulation results were in agreement with experimental evidence, summarized as follows: In the limit of low magnetic moment $m < 3.7\times10^{-16}$ A·m^2, magnetic nanoparticles did not linearly arrange along the direction of the magnetic field but formed aggregates. At magnetic moment $m > 1.5\times10^{-15}$ A·m^2 and volume fraction $\varphi <$ 0.02%, the formation effect of nanochains, which consisted of individual particles, first enhanced and then remained unchanged with increasing magnetic moment. For magnetic moment $m > 7.3\times10^{-15}$ A·m^2 and volume fraction $\varphi > 1\%$, nanochains gradually coarsened into nanobundles with increasing volume fraction. The results may lay the foundation for researching other assembled structures consisting of building blocks.

Supplementary Information The online version contains supplementary material available at https://doi.org/10.1007/s11051-021-05203-7.

Funding This work was supported by the National Natural Science Foundation of China (No. 11672041).

Compliance with ethical standards

Conflict of interest The authors declare no competing financial interests.

References

Bertoni G, Torre B, Falqui A, Fragouli D, Athanassiou A, Cingolani R (2011) Nanochains formation of superparamagnetic nanoparticles. J Phys Chem C 115: 7249–7254. https://doi.org/10.1021/jp111235n

Chen YP, Li SC, Wei XB, Tang RZ, Zhou ZN (2018) Infrared extinction and microwave absorption properties of hybrid Fe_3O_4@SiO_2@Ag nanospheres synthesized via a facile seed-mediated growth route. Nanotechnology 29:375703. https://doi.org/10.1088/1361-6528/aace23

Enomoto Y, Oba K, Okada M (2003) Simulation study on microstructure formations in magnetic fluids. Physica A 330:496–506. https://doi.org/10.1016/S0378-4371(03)00624-1

Furst EM, Gast AP (2000) Dynamics and lateral interactions of dipolar chains. Phys Rev E 62:6916–6925. https://doi.org/10.1103/PhysRevE.62.6916

He L, Hu Y, Han X, Lu Y, Lu Z, Yin Y (2011) Assembly and photonic properties of superparamagnetic colloids in complex magnetic fields. Langmuir 27:13444–13450. https://doi.org/10.1021/la2026768

He L, Wang M, Ge J, Yin Y (2012) Magnetic assembly route to colloidal responsive photonic nanostructures. Acc Chem Res 45:1431–1440. https://doi.org/10.1021/ar200276t

Helseth LE (2005) Self-assembly of colloidal pyramids in magnetic fields. Langmuir 21:7276–7279. https://doi.org/10.1021/la051140v

Hu Y, He L, Yin Y (2011) Magnetically responsive photonic nanochains. Angew Chem Int Edit 50:3747–3750. https://doi.org/10.1002/anie.201100290

Islam MF, Lin KH, Lacoste D, Lubensky TC, Yodh AG (2003) Field-induced structures in miscible ferrofluid suspensions with and without latex spheres. Phys Rev E 67:021402. https://doi.org/10.1103/PhysRevE.67.021402

Kamble RB, Mathe VL (2008) Nanocrystalline nickel ferrite thick film as an efficient gas sensor at room temperature. Sensors Actuators B Chem 131:205–209. https://doi.org/10.1016/j.snb.2007.11.003

Kralj S, Makovec D (2015) Magnetic assembly of superparamagnetic iron oxide nanoparticle clusters into nanochains and nanobundles. ACS Nano 9:9700–9707. https://doi.org/10.1021/acsnano.5b02328

Lalatonne Y, Richardi J, Pileni MP (2004) Van der Waals versus dipolar forces controlling mesoscopic organizations of magnetic nanocrystals. Nat Mater 3:121–125. https://doi.org/10.1038/nmat1054

Laughlin DE, Lu B, Hsu YN, Zou J, Lambeth D (2000) Microstructural and crystallographic aspects of thin film recording media. IEEE Trans Magn 36:48–53. https://doi.org/10.1109/20.824424

Malik V, Petukhov AV, He L, Yin Y (2012) Colloidal crystallization and structural changes in suspensions of silica/magnetite core–shell nanoparticles. Langmuir 28:14777–14783. https://doi.org/10.1021/la301942t

Miller JS, Drillon M (2005) Magnetism: molecules to materials V. Wiley, Weinheim, pp 189–222

Ohno K, Sakaue M, Mori C (2018) Magnetically responsive assemblies of polymer-brush-decorated nanoparticle clusters that exhibit structural color. Langmuir 34:9532–9539. https://doi.org/10.1021/acs.langmuir.8b02073

Peng X, Min Y, Ma T, Luo W, Yan M (2009) Two-dimensional Monte Carlo simulations of structures of a suspension comprised of magnetic and nonmagnetic particles in uniform magnetic fields. J Magn Magn Mater 321:1221–1226. https://doi.org/10.1016/j.jmmm.2008.11.011

Ravi S (2020) High curie temperature and room temperature magnetoresistance in Pr_2FeCrO_6 material for spintronics applications. Mater Lett 278:128448. https://doi.org/10.1016/j.matlet.2020.128448

Ravi S, Prabvin VS (2013) Nanostructured copper oxide synthesized by a simple bio-molecule assisted route with wide bandgap. Nanosci Nanotechnol Lett 5:879–882. https://doi.org/10.1166/nnl.2013.1632

Ravi S, Shashikanth FW (2017) Preparation of Mn doped CeO_2 nanoparticles with enhanced ferromagnetism. Mater Chem Phys 194:37–41. https://doi.org/10.1016/j.matchemphys.2017.03.032

Richardson JM, Jones CW (2009) Leached nickel promotes catalysis using supported Ni(II) complex precatalysts in kumada-corriu reactions. J Mol Catal A Chem 297:128–134. https://doi.org/10.1016/j.molcata.2008.09.021

Satoh A, Chantrell RW, Kamiyama SI, Coverdale GN (1996) Three dimensional Monte Carlo simulations of thick chainlike clusters composed of ferromagnetic fine particles. J Colloid Interface Sci 181:422–428. https://doi.org/10.1006/jcis.1996.0399

Satoh A, Coverdale GN, Chantrell RW (2000) Stokesian dynamics simulations of ferromagnetic colloidal dispersions subjected to a sinusoidal shear flow. J Colloid Interface Sci 231:238–246. https://doi.org/10.1006/jcis.2000.7118

Tran VT, Zhou H, Lee S, Hong SC, Kim J, Jeong SY, Lee J (2015) Magnetic-assembly mechanism of superparamagneto-plasmonic nanoparticles on a charged surface. ACS Appl Mater Interfaces 7:8650–8658. https://doi.org/10.1021/acsami.5b00904

Wang H, Chen QW, Sun YB, He MY (2010) Synthesis of superparamagnetic colloidal nanochains as magnetic-responsive bragg reflectors. J Phys Chem C 114:19660–19666. https://doi.org/10.1021/jp1081752

Wang M, He L, Yin Y (2013a) Magnetic field guided colloidal assembly. Mater Today 16:110–116. https://doi.org/10.1016/j.mattod.2013.04.008

Wang M, He L, Hu Y, Yin Y (2013b) Magnetically rewritable photonic ink based on superparamagnetic nanochains. J Mater Chem C 1:6151–6156. https://doi.org/10.1039/C3TC30765D

Xue X, Furlani EP (2014) Template-assisted nano-patterning of magnetic core–shell particles in gradient fields. Phys Chem Chem Phys 16:13306–13317. https://doi.org/10.1039/c4cp01563k

Xue X, Furlani EP (2015) Analysis of the dynamics of magnetic core–shell nanoparticles and self-assembly of crystalline superstructures in gradient fields. J Phys Chem C 119:5714–5726. https://doi.org/10.1021/jp513025w

Xue X, Liu K, Furlani EP (2017) Theoretical study of the self-assembly and optical properties of 1D chains of magnetic–plasmonic nanoparticles. J Phys Chem C 121:9489–9496. https://doi.org/10.1021/acs.jpcc.7b00824

Ye M, Zorba S, He L, Hu Y, Maxwell RT, Farah C, Zhang Q, Yin Y (2010) Self-assembly of superparamagnetic magnetite particles into peapod-like structures and their application in optical modulation. J Mater Chem 20:7965–7969. https://doi.org/10.1039/C0JM02001J

Yuan J, Xu Y, Müller Axel HE (2011) One-dimensional magnetic inorganic-organic hybrid nanomaterials. Chem Soc Rev 40:640–655. https://doi.org/10.1039/C0CS00087F

Zhang Z, Duan H, Li S, Lin Y (2010) Assembly of magnetic nanospheres into one-dimensional nanostructured carbon hybrid materials. Langmuir 26:6676–6680. https://doi.org/10.1021/la904010y